



International Journal of Environment and Geoinformatics (IJEGEO) is an international, multidisciplinary, peer reviewed, open access journal.

The Methodology and Results from Ground Validation of Satellite Observations at Gas Flaring Sites in Nigeria

Barnabas O. MORAKINYO, Samantha LAVENDER, Victor ABBOTT

Chief in Editor

Prof. Dr. Cem Gazioğlu

Co-Editors

Prof. Dr. Dursun Zafer Şeker, Prof. Dr. Şinasi Kaya,

Prof. Dr. Ayşegül Tanık and Assist. Prof. Dr. Volkan Demir

Editorial Committee (September 2021)

Assoc. Prof. Dr. Abdullah Aksu (TR), Assit. Prof. Dr. Uğur Algancı (TR), Prof. Dr. Bedri Alpar (TR), Assoc. Prof. Dr. Aslı Aslan (US), Prof. Dr. Levent Bat (TR), Prof. Dr. Paul Bates (UK), İrşad Bayırhan (TR), Prof. Dr. Bülent Bayram (TR), Prof. Dr. Luis M. Botana (ES), Prof. Dr. Nuray Çağlar (TR), Prof. Dr. Sukanta Dash (IN), Dr. Soofia T. Elias (UK), Prof. Dr. A. Evren Erginal (TR), Assoc. Prof. Dr. Cüneyt Erenoğlu (TR), Dr. Dieter Fritsch (DE), Prof. Dr. Çiğdem Göksel (TR), Prof. Dr. Lena Halounova (CZ), Prof. Dr. Manik Kalubarme (IN), Dr. Hakan Kaya (TR), Assist. Prof. Dr. Serkan Kükrer (TR), Assoc. Prof. Dr. Maged Marghany (MY), Prof. Dr. Michael Meadows (ZA), Prof. Dr. Nebiye Musaoğlu (TR), Prof. Dr. Masafumi Nakagawa (JP), Prof. Dr. Hasan Özdemir (TR), Prof. Dr. Chryssy Potsiou (GR), Prof. Dr. Erol Sarı (TR), Prof. Dr. Maria Paradiso (IT), Prof. Dr. Petros Patias (GR), Prof. Dr. Elif Sertel (TR), Prof. Dr. Nüket Sivri (TR), Prof. Dr. Füsün Balık Şanlı (TR), Prof. Dr. Uğur Şanlı (TR), Duygu Ülker (TR), Prof. Dr. Seyfettin Taş (TR), Assoc. Prof. Dr. Ömer Suat Taşkın (TR), Assist. Prof. Dr. Tuba Ünsal (TR), Dr. Manousos Valyrakis (UK), Dr. İnese Varna (LV), Dr. Petra Visser (NL), Prof. Dr. Selma Ünlü (TR), Assoc. Prof. Dr. Oral Yağcı (TR), Prof. Dr. Murat Yakar (TR), Assoc. Prof. Dr. İ. Noyan Yılmaz (AU); Assit. Prof. Dr. Sibel Zeki (TR)

Abstracting and Indexing: TR DIZIN, DOAJ, Index Copernicus, OAJI, Scientific Indexing Services, International Scientific Indexing, Journal Factor, Google Scholar, Ulrich's Periodicals Directory, WorldCat, DRJI, ResearchBib, SOBIAD

Research Article

The Methodology and Results from Ground Validation of Satellite Observations at Gas Flaring Sites in Nigeria

Barnabas O. Morakinyo^{1,2,3,4*} , Samantha Lavender^{2,3} , Victor Abbott² 

¹ Baze University, Faculty of Environmental Sciences, Department of Surveying & Geoinformatics, Abuja, NIGERIA

² University of Plymouth, Faculty of Science & Technology, School of Marine Science & Engineering, Plymouth, UK

³ Pixalytics Ltd, 1 Davy Rd, Tamar Science Park, Plymouth, UK

⁴ ARGANS Ltd, 1 Davy Rd, Tamar Science Park, Plymouth, UK

*B. O. Morakinyo

E-mail: barnabas.ojo@bazeuniversity.edu.ng

Received: 09 Jan 2020

Accepted: 14 Feb 2021

How to cite: Morakinyo et al., (2021). The Methodology and Results from Ground Validation of Satellite Observations at Gas Flaring Sites in Nigeria, *International Journal of Environment and Geoinformatics (IJECEO)*, 8(3):290-300. doi. 10.30897/ijegeo.749664

Abstract

This study examines the importance of ground validation to Landsat 5 Thematic Mapper (TM) and Landsat 7 Enhanced Thematic Mapper Plus (ETM+) observations at 2 gas flaring sites in Rivers State, Niger Delta, Nigeria. 12 Landsat imagery (3 Landsat 5 TM and 9 Landsat 7 ETM+) data acquired from 25/03/1987 to 08/03/2013 with < 5 % cloud contamination were used. Both sites are located within a single Landsat scene (Path 188, Row 057). Ground measurements and observations at both sites took place from (04/08/2012-21/09/2012) and (05/08/2019-22/09/2019). Parameters measured are coordinates of points and features, air temperature and relative humidity; and photographs of locations and features were taken. Both air temperature and relative humidity were measured at 3 different levels above the ground surface at 1 minute interval. The results show that the locational error of points and features from Landsat data and fieldwork measurements give negligible difference of 1.0×10^{-6} to 7.3×10^{-6} . Also, 4 classes of land use and land cover (LULC) types retrieved from Landsat data are the same with those observed on site during ground measurements. The air temperature (AT) recorded and Land Surface Temperature (LST) retrieved from Landsat data for both sites show that the closer the distance to the flare, the higher the temperature and vice versa. Results show that the spatial variability in ground AT and derived LST from Landsat data differs within 0.8 to 6.0 K because AT is different from LST. Based on the results acquired, it can be concluded that ground validation is essential and required for maximum utilization and exploitation of remote sensing technology applications.

Keywords: Ground validation, satellites, methodology, imageries, gas flaring, Niger Delta.

Introduction

Multi-temporal imagery is generally geometrically and radiometrically accurate, but the residual noise arising from removal of clouds and other atmospheric and electronic effects can produce irregularity that must be mitigated to properly exploit the remote sensing information (Militino et al., 2018). Hence, causing distortion and missing of data in satellite imagery. In remote sensing, ground validation (through the collection of field data) is especially important to relate image data to real features and materials on the ground (Brown, 1996; Avşar et al., 2016; Esetlili et al., 2018). More specifically, ground validation may refer to a process in which a pixel on a satellite image is compared to what is on ground in reality (at a matching time) in order to verify what the pixel is showing. Ground-based data is required for validation of any remote sensing technique, whether it is for land surface or seabed mapping, no matter the spatial resolution or source (Serpetti et al., 2011; Gazioğlu et al., 2002, 2017). Furthermore, remote sensing instruments may not be able to identify all the features at the time the satellite passes over a given area due to for example spectral ambiguity or cloud cover. Therefore, ground validation can also be an effective means to fill in the features that

were missing or could not be easily identified through the imagery (Vega et al., 2011).

Ground validation usually involves performing surface observations and measurements of various properties of the features that are being studied. It also involves taking the coordinates of features and comparing those with the coordinates of the corresponding pixel being studied to understand and analyse the location errors and how these may affect a particular study (Sadd et al., 2015; Büyüksalih et al., 2009; Vega et al., 2011). Ground validation is also important in the initial supervised classification of an image and helps with validation of the atmospheric correction. Other purposes of acquiring ground validation data include calibration of remote sensing sensors; and development of multi-satellite remote sensing interpretation (Morakinyo, 2015; Pressler and Walker, 1999).

Some researchers on ground validation of satellite data include Militino et al. (2018) who merged Moderate Resolution Imaging Spectroradiometer (MODIS) data with ground data for gap-filling and smoothing of satellite data for the purpose of eliminating irregularities. Yeboah et al. (2017) and Pareta (2014) acquired Landsat 5 Thematic Mapper (TM) data, Landsat 7 Enhanced Thematic Mapper (ETM+) data, and field data for land

use and land cover (LULC) studies and change detection analysis. In addition, Landsat 5 TM data, SPOT High Resolution Visible (HRV) data and ground survey data were combined for mapping and classification of high relief terrain (Franklin, 1991); and habitat land cover (LC) (Matthew, 1991). Otukey and Blaschke (2012) worked on comparison of Land Surface Temperature (LST) retrieved from Landsat 7 ETM+ low gain and high gain thermal infrared band data, and that of ground data (Celik et al., 2019; Sutariya et al., 2021).

Furthermore, Metz et al. (2017) used air temperature ground data to check and improve the predicted LSTs obtained from MODIS LST data. Coll et al. (2010) worked on validation of Landsat 7 ETM+ data thermal band calibration and atmospheric correction using ground based measurements with two approaches of obtaining the atmospheric correction parameters from local-radiosonde profiles and from Atmospheric Correction Parameter (ATM CORR) Calculator. Ifatimehin and Adeyemi (2008) examined the difference between LSTs retrieved from Landsat 5 TM data and that of the in-situ data. Finally, Dung et al. (2008) reported only fieldwork activities on measurement of air temperature (AT) carried out at 6 flare sites in the Niger Delta.

It is difficult to make in-situ measurements coincident with image acquisition, and the measurement scales and properties of the surface recorded are fundamentally different. Another problem of ground validation is the lack of an absolute scale of truth, or correctness (Thomas et al., 2007; Islam, et al., 2016). Therefore, relationships developed between in-situ and remotely sensed measurements often come with extensive sets of qualifiers or more usually are specific to a particular image acquisition (Smith et al., 2009). Ground validation requires local knowledge of the site, and its landscape (Al-Abdulrazzak and Pauly, 2014); and lack of local

knowledge may invalidate the ground validation intended (Garibaldi et al., 2014). For this research, fieldwork activities were carried out with the aim of ground validation at 2 gas flaring sites (Eleme Petroleum Refinery Company II and Onne Flow Station) both in Rivers State, Nigeria.

The gaps before this research is that in the Niger Delta, limited research into ground validation of satellite data (Landsat 5 TM and Landsat 7 ETM+) applied for mapping of flaring sites has been published to date, and no study applied the methodology discussed in this paper. The basis for this research is the concept that using satellite imagery with field survey data would result in significantly better analyses than using only satellite data alone. Therefore, the 3 basic research questions for this study are: (1) What is the locational error/accuracy of established features obtained from satellite data and those measured in the field in the Niger Delta? (2) What are the LULC types at the flaring sites, and the pattern of plumes observed from gas flaring in the Niger Delta? (3) What is the spatial and temporal variability in satellite derived LST and AT? Based on these questions, the primary aim of this study is to create a Nigeria-focused methodology for ground validation of Landsat 5 TM and Landsat 7 ETM+ satellite based sensors observations at gas flaring sites. The specific objectives set for these research questions are: (1) Comparison of coordinates of features recorded from Landsat 5 TM and Landsat 7 ETM+ data with those measured on sites; (2) Comparison of classified LULC types retrieved from Landsat 5 TM and Landsat 7 ETM+ data and those observed at the flaring sites; and close observations of the pattern of plumes at the flaring sites; (3) Comparison of spatial variability in Landsat 5 TM and Landsat 7 ETM+ derived LSTs and AT measured at the sites.

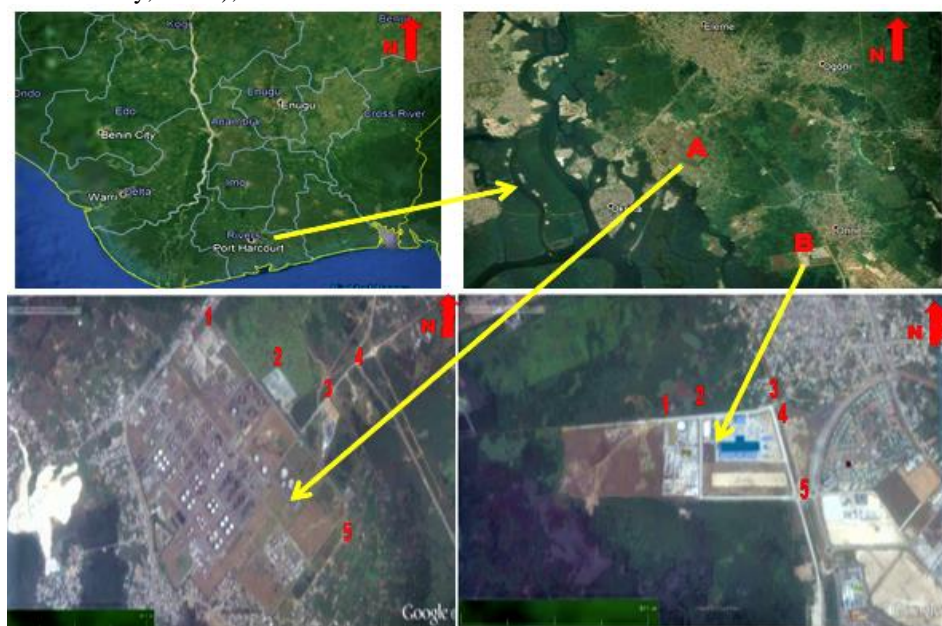


Figure 1: A) Eleme Refinery II Petroleum Company; B) Onne Flow Station sites in Rivers State, Niger Delta, Nigeria (Source: Google Earth, 2020)

Study Area

Ground validation of satellite data accessed for this study is limited to 2 flare sites (Eleme Refinery II Petroleum Company (hereafter called Eleme Refinery II) and Onne Flow Station located in Eleme Local Government Area (Figure 1), Rivers State of the Niger Delta, Nigeria between Latitude 04° 40' to 05 °55' N and Longitude 06° 50' to 07° 05' E (Morakinyo et al., 2019). Eleme Refinery II was built in 1988 and commissioned in 1989 (Morakinyo, 2015) in Eleme town. It is about 2.2 by 1.3 km in size with a flare stack of about 65 m height (Morakinyo, 2015). Eleme Refinery II complex is situated at about 70 km from the Eastern part of Port Harcourt, Rivers State capital. Onne Flow Station was built in 2010 with about 175 by 130 m in size; and a flare stack (3 pipes connected to a source) being about 3.5 m in height from the ground (Figure 1 B) (Morakinyo, 2015). It is about 20 km to the South-East of Eleme Refinery II.

Materials and Methods

3 types of data involved in this research are satellite data (Landsat 5 TM and Landsat 7 ETM+), fieldwork data (In-situ data) and meteorological data. The methods adopted for the acquisition of field data is discussed under methodology. 3 imagery of Landsat 5 TM and 9 imagery of Landsat 7 ETM+ dated 25/03/1987 to 08/03/2013 used were downloaded from the USGS Earth Resources Observation and Science (EROS) Data Centre website (<http://earthexplorer.usgs.gov/>) using the Glovis/Earth Explorer interface. The scenes with < 5% contamination were selected for the research (Table 1); and both sites are located within a single Landsat scene (Path 188, Row 057). Landsat 5 TM images are acquired in 7 spectral bands while Landsat 7 ETM+ is acquired in

8 spectral bands; and both have similar spatial resolution of 30 m for bands 1-5 and 7. Band 8 for Landsat 7 ETM+ is panchromatic with a spatial resolution of 15 m. The spatial resolution for Landsat 5 TM band 6 (thermal infrared) is 120 m while for Landsat 7 ETM+ is 60 m but both are resampled to 30 m pixels (Morakinyo, 2015; Chander and Markham, 2003). L1T is the processing level for all the imageries, which means systematic radiometric and geometric correction using ground control points (GCPs), and digital elevation model (DEM) has been applied. The problem of Scan Line Correction (SLC-off mode) with Landsat 7 sensor which started from 2004 that lead to loss of part of data in the imageries (Chen et al., 2012) was reduced to a minimum by setting one of the criteria for the selection of flare sites as the availability of data covering each facility.

Meteorological Data

The nearest meteorological station to the 2 flaring sites examined is about 50 km away, and is located at Port Harcourt International Airport, Rivers State. This meteorological data are used to evaluate the phenomena of the atmosphere, especially weather and weather conditions of Port Harcourt and its environs, in relation to the acquired study data. The minimum data requirements for analysis of the meteorological effects in Port Harcourt and its environs are daily observation of the meteorological parameters. The meteorological data (AT: minimum and maximum), relative humidity, wind direction, wind speed, solar radiation, rainfall, and sunshine; from 2000 to 2019) available for the study were provided on monthly basis and were collected from the Nigeria Meteorological Agency (NMA), Lagos, Nigeria. Table 2 shows the average daily air temperature measured at Port Harcourt International Airport Meteorological station from 2000 to 2019.

Table 1: Details of Landsat 5 TM & Landsat 7 ETM+ datasets used.

S/N	Image Identity No.	Date	UTC Time (h: m)	Path/row	Processing Level
1.	LT51880571987084XXX02	25-03-1987	09:07	188/057	L1T
2.	LT51880571990356XXX03	22-12-1990	09:10	188/057	L1T
3.	LT51880571991007XXX03	07-01-1991	09:09	188/057	L1T
4.	LE71880572000352EDC00	17-12-2000	09:35	188/057	L1T
5.	LE71880572003008SGS00	08-01-2003	09:33	188/057	L1T
6.	LE71880572004331ASN00	26-11-2004	09:34	188/057	L1T
7.	LE71880572005013ASN00	13-01-2005	09:34	188/057	L1T
8.	LE71880572007355ASN00	21-12-2007	09:35	188/057	L1T
9.	LE71880572008326ASN00	21-11-2008	09:34	188/057	L1T
10.	LE71880572010107ASN00	17-04-2010	09:37	188/057	L1T
11.	LE71880572012225ASN00	12-08-2012	09:40	188/057	L1T
12.	LE71880572013067ASN00	08-03-2013	09:41	188/057	L1T

Table 2: Average daily Air Temperature (K) at Port Harcourt International Airport, Rivers State (2000-2019).

	Jan.	Feb.	March	April	May	June	July	August	Sept.	Oct.	Nov.	Dec.
Temperature (K°)	300.8	302.1	301.7	301.3	300.4	299.4	298.4	298.2	298.7	299.2	300.5	300.4

*Source: NMA, Lagos

Methodology

Ground Measurements

For this research, on 27 July 2012, both sites were visited for the purposes of a reconnaissance survey; and it was discovered that (1) Some areas within each site are swampy which made them difficult to walk upon; (2) Direct or open access would not be allowed into the 2 flaring sites; (3) The use of surveying instruments openly at both sites would be difficult because the local communities could become hostile which can lead to loss of life and that of surveying instruments. The surroundings consist of a mixture of oil, water and open ground without grass; especially close to the gas flaring stack. Also, far away from the stack, changes in land cover were noticed; the ground was covered with grass and other vegetation (trees) at about 180 m away from the flaring stacks. The reconnaissance survey helped to choose Saturday 4 August 2012 as the starting date for the first actual fieldwork.

Fieldwork activities were carried out to collect data for a ground validation of Landsat 5 TM and Landsat 7 ETM+ data. It involved physical inspection and ground measurements at Eleme Refinery II and Onne Flow

Station. The variables measured were the coordinates of ground points/some selected features within 480 m² around the flare at 30 m intervals; AT and relative humidity. Photographs were taken of identified locations with evidence of the impacts of gas flares. The first fieldwork observations and measurements of 2 sets took place at both sites in August and September, 2012, during a period of six weeks (04/08-21/09/2012). The weather conditions were similar throughout this period being clear sky, dry and air temperatures of around 20 °C. Distance measurement started at 30 m away from the flare stack at both sites. 8 lines were projected from both flare stacks in order to obtain the detailed features surrounding the flaring sources (Figure 2). A distance of 30 m was measured with a steel tape and the author paced it to know the exact number of steps that are equivalent to the 30 m distance measured with the steel tape in order to avoid the open use of surveying instruments. The uncertainty in the initial taped 30 m measured is ± 0.015 m. Each point measured at every 30 m interval was marked with a permanent object to enable proper identification during the second visit, and for future reference; each line was made up of 8 points with a total distance of 240 m.



Figure 2: Location of gas flaring stack and field measurements of selected points (in red) at 1) Eleme Refinery II; 2) Onne Flow Station, (Google Earth image overlaid with GPS derived points).

Table 3: Mean Air Temperature (K) for Eleme Refinery II and Onne Flow Station

Eleme II	30 m	60 m	90 m	120 m	150 m	180 m	210 m	240 m
L1	323.8	320.0	318.2	317.3	316.6	316.2	315.4	314.4
L2	323.6	320.0	318.4	317.5	316.7	316.2	314.6	314.0
L3	323.1	319.5	318.4	316.0	316.6	316.2	315.0	313.7
L4	323.9	322.2	317.9	317.4	316.3	316.2	314.8	315.8
L5	322.8	320.3	318.4	317.3	316.5	315.9	315.1	313.9
L6	323.1	320.7	319.1	317.8	317.2	315.9	315.0	314.3
L7	323.8	323.0	318.7	317.3	317.4	317.0	315.1	314.2
L8	323.1	320.8	319.3	318.0	317.2	316.8	315.0	314.3
Onne								
L1	323.3	320.7	319.1	318.4	317.6	316.9	315.6	314.8
L2	322.4	319.8	318.3	317.5	316.9	316.5	315.0	314.5
L3	321.3	319.1	317.7	316.3	315.8	315.2	314.8	314.9
L4	322.5	321.2	318.6	317.6	317.2	316.0	315.0	314.5
L5	321.2	320.0	318.3	317.5	316.6	316.0	314.5	313.9
L6	321.9	320.8	319.0	317.4	316.4	315.8	314.6	313.9
L7	322.4	322.0	319.2	317.8	316.8	316.3	314.5	314.1
L8	322.5	320.8	318.8	317.6	317.0	316.3	314.5	314.0

Land Use and Land Cover Classification and Retrieval of LST with atmospherically corrected Landsat 5 TM and Landsat 7 ETM+ data.

The methods adopted are:

(1) Verification of geo-location points using Google Earth. 5 ground control points each were selected over Eleme Refinery II and Onne Flow Station sites and measured with GPS on site during the fieldwork. 12 imageries (3 Landsat 5 TM and 9 Landsat 7 ETM+) were uploaded into ArcGIS and the selected ground control points (GCPs) were identified.

(2) MATLAB code was used for data processing and for removal of zero or out of range values from the data and their replacement with not a number (nan) to avoid divide by zero errors in calculations.

(3) Radiometric calibration of the thermal band (6) of the data by converting the Digital Number (DN) values recorded into top of atmosphere (TOA) radiance or temperature values based on sensor calibration parameters provided within the metadata files from USGS (Chander and Markham, 2003; NASA, 2002) using equation 1

$$L_{\lambda} = ((LMAX_{\lambda} - LMIN_{\lambda}) / (QCALMAX - QCALMIN)) \times (QCAL - QCALMIN) + LMIN_{\lambda} \quad (Eq.1)$$

Where:

L_{λ} = Spectral Radiance at the sensor's aperture in $Wm^{-2}sr^{-1}\mu m^{-1}$;

QCAL = The quantized calibrated pixel value in DN;

$LMIN_{\lambda}$ = The spectral radiance that is scaled to QCALMIN in $Wm^{-2}sr^{-1}\mu m^{-1}$;

$LMAX_{\lambda}$ = The spectral radiance that is scaled to QCALMAX in $Wm^{-2}sr^{-1}\mu m^{-1}$;

QCALMIN = The minimum quantized calibrated pixel value (corresponding to $LMIN_{\lambda}$) in DN = 1 for LPGS (a processing software version) products;

QCALMAX = The maximum quantized calibrated pixel value (corresponding to $LMAX_{\lambda}$) in DN = 255.

(4) Correction of the atmospheric effects for multispectral bands (1-4) and thermal band. The atmospheric correction parameters, upwelling radiance (L_u), downwelling radiance (L_d), and transmittance (τ) were obtained from Atmospheric Correction Parameters (ATMCORR) Calculator, a National Aeronautics and Space Administration (NASA) web tool developed by Barsi et al. (2005). Dark Object Subtraction (DOS) method (Kaufman et al., 2000) was adopted for the correction of atmospheric effects on the multispectral bands (1-4).

(5) LULC classification: The cluster analysis was performed with the cloud-masked reflectance (bands 1-4) to give 4 (vegetation, soil, built up area and water) LC types for both sites (Figure 3) (Maaharjan, 2018).

(6) Retrieval of LST: The theoretical basis for the LST measurement is Plank's radiation function, formulated as:

$$B(\lambda, T) = \frac{C_1 \lambda^{-5}}{\pi (\exp(C_2/\lambda T) - 1)} \quad (Eq.2)$$

Where:

$B(\lambda, T)$ = Spectral radiance of a blackbody in $Wm^{-2}sr^{-1}\mu m^{-2}$; λ = Wavelength (m);

T = Temperature in Kelvin; C_1 = The first spectral constant = $3.741775 \times 10^{-22} Wm^2$;

C_2 = The second spectral constant $1.4388 \times 10^{-2} mK$; π (pi) = constant = 3.142 (Qin et al., 2011).

When $B(\lambda, T)$ is measured generally by a thermal sensor, the surface-leaving radiance (L_{λ}) can be computed by inverting the Planck's radiance function as follows (Figure 3):

$$L_{\lambda} = \frac{C_2}{\lambda \ln[(C_1/\lambda^5 B(\lambda, T)) + 1]} \quad (Eq. 3)$$

The approach for the calculation of LST, by first calculating L_{λ} and substituting it into the Planck function and inverting the function to get the LST was adopted for the study (Figure 3) (Morakinyo, 2015; Coll, 2010). The formula for computing L_{λ} is:

$$L_{\lambda} = ((L_s - L_u) / \epsilon \tau) - ((1 - \epsilon) / \epsilon) \times L_d \quad (Wm^{-2}sr^{-1}\mu m^{-1}) \quad (Eq.4)$$

The L_u , L_d , and τ were applied to the calibrated at-sensor radiance band 6 (high gain) data to compute the L_{λ} .

Where,

L_s = Radiometrically corrected Landsat thermal band 6 radiance (high gain);

L_u = Upwelling radiance; L_d = Downwelling radiance;

τ = Atmospheric transmission; ϵ = emissivity.

L_u , L_d , and τ are atmospheric correction parameters for the Landsat thermal band.

LST was derived using equation 5.

$$LST = \frac{K_2}{\ln((K_1/L_{\lambda}) + 1)} \quad (Eq. 5)$$

Where, K_1 and K_2 are thermal band calibration constants calculated for the Landsat sensor characteristics.

For Landsat 5 TM, $K_1 = 607.76 (Wm^{-2}sr^{-1}\mu m^{-1})$ and $K_2 = 1260.56 (K)$; and

For Landsat 7 ETM+, $K_1 = 666.09 (W m^{-2} sr^{-1}\mu m^{-1})$ and $K_2 = 1282.71 (K)$.

The ground based methods adopted for this research improve the quality of the satellite images in the following ways:

1. Assessment of the locational errors of points and features retrieved from Landsat 5 TM and Landsat 7 ETM+ images is possible;
2. Classification and clarification of LULC types retrieved from satellite images and for some specific features that are missing in Landsat 7 ETM+ images due to problem of SLC-off mode is ascertained;
3. AT measured and those obtained from meteorological agency provided primary information about temperature of the 2 sites;

4. The pattern of plumes observed during field measurements also support the LSTs retrieved from Landsat data;

5. The 2 site visits also clarify the changes recorded in LSTs retrieved from one imagery to another.

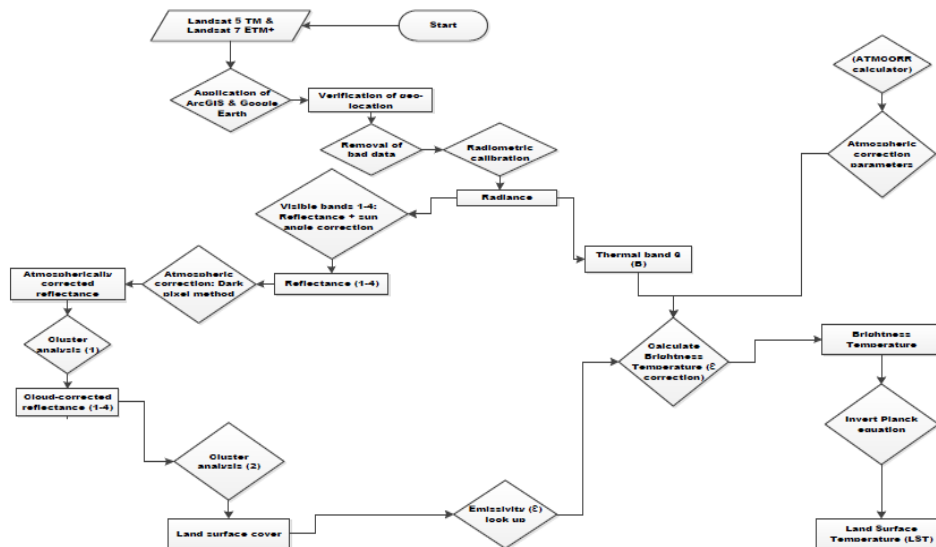


Figure 3: Methodological workflow for the processing of Landsat 5 TM and Landsat 7 ETM+ data for LULC classifications and retrieval of LST.

Table 4: Locational error/accuracy of established ground control points

Point	Field data		L5 TM & L7 ETM+		Remarks (See Figure 1)
	Latitude (θ)	Longitude (λ)	Latitude (θ)	Longitude (λ)	
Eleme II					
1.	4.7708333	7.1048999	4.7708333	7.1049000	A sharp edge of the refinery complex fence
2.	4.7671556	7.1112750	4.7671555	7.1112750	A sharp edge of a structure before entering the refinery complex
3.	4.7664583	7.1160167	4.7664583	7.1160166	A point on the road (leading to the refinery) in front of a structure
4.	4.7611083	7.1028222	4.7611083	7.1028222	3 roads at meeting point i.e. T-junction point
5.	4.7529833	7.1029222	4.7529833	7.1029222	A polluted point outside the refinery complex, on the East side of the complex
Onne					
1.	4.7170833	7.1386056	4.7170833	7.1386056	A point on the road bounding the flow station
2.	4.7172778	7.1417445	4.7172778	7.1417444	Another point on the road bounding the flow station
3.	4.7182277	7.1480195	4.7182278	7.1480194	A point on the ground at a junction
4.	4.7185278	7.1490888	4.7185278	7.1490889	A point on the major road at the edge of a structure
5.	4.7117138	7.1501417	4.7117139	7.1501417	A point on a small road that linked 2 major roads

Results and Discussion

Evaluation of locational error/accuracy of established points/features

The coordinates of controls obtained from Landsat 5 TM and Landsat 7 ETM+ imageries, and fieldwork were compared and a negligible difference was found (1.0×10^{-6} to 7.3×10^{-6} m) (Table 4).

Land Use and Land Cover types and the pattern of plumes observed from gas flaring

For both Eleme Refinery II and Onne Flow Station flaring sites, it was observed during ground measurement that 4 LULC types recorded (vegetation, soil, built-up area and water) are the same with those retrieved from

Landsat 5 TM and Landsat 7 ETM+ data (Figure 4). Also, it was observed that the plume from the flare stacks moves outwardly as shown in Figure 4. Furthermore, it was clear that during 2019 visit to both sites the volume of the visible flame was greater than that of 2012 visit. This was supported by detection of the higher temperatures being radiated from the flame. The noise coming out from the burning of gas on 2019 visit was louder than that of 2012 visit. This could be as a result of the increase in the numbers of barrels of crude oil that were undergoing refining processes at Eleme Refinery II; and also the increase in the barrels of crude oil stored at the Onne Flow Station.

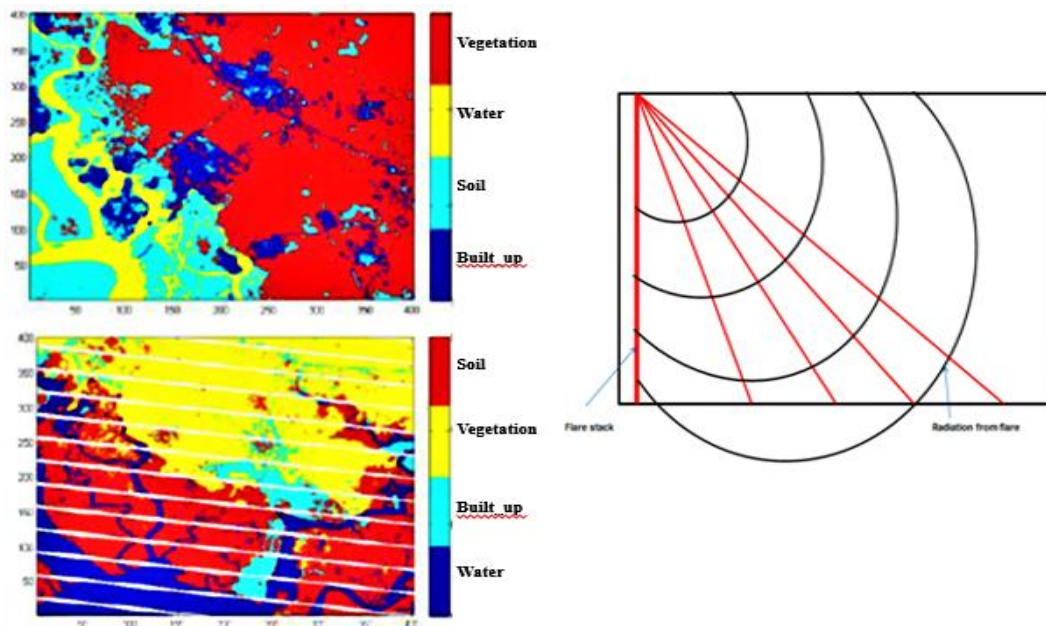
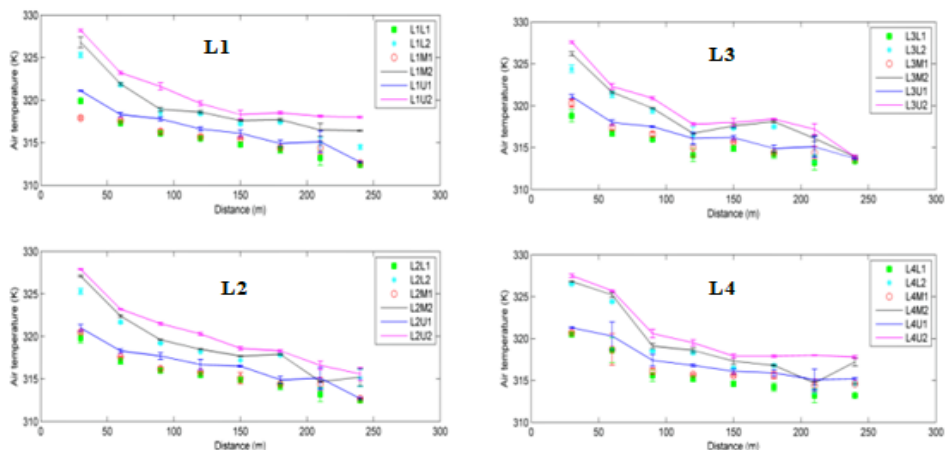


Figure 4: LULC types: Upper left (Eleme Refinery II); lower left (Onne Flow Station); and Right: Pattern of plumes

Air Temperature measured in the field

The AT results for both sites show that the closer the distance to the flare stack, the higher the AT measured and vice-versa (Table 3); The upper reading values are the highest and vice-versa. This is supported by Dung et al. (2008) who reported that the air, soil and leaf temperatures increased within 110 m away from 6 flare sites investigated; and that the closer to the flare, the higher the temperature and vice versa. The mean AT measured (Transect lines 1 to 8) for both sites are presented in Figures 5 and 6. Abbreviations used in the figure keys are explained below with L1 to L8 representing lines number 1 to 8:

- L1 (Lower 1) = AT reading at 1 m above the ground for 2012 set of data;
- L2 (Lower 2) = AT reading at 1 m above the ground for 2019 set of data;
- M1 (Middle 1) = AT reading at 1.5 m above the ground for 2012 set of data;
- M2 (Middle 2) = AT reading at 1.5 m above the ground for 2019 set of data;
- U1 (Upper 1) = AT reading at 2 m above the ground for 2012 set of data;
- U2 (Upper 2) = AT reading at 2 m above the ground for 2019 set of data.



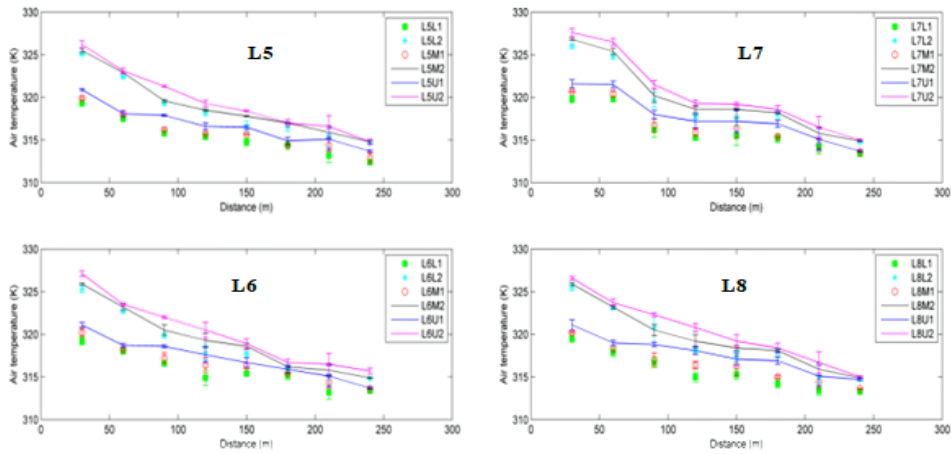


Figure 5: Air temperature at Eleme Refinery II (L1-L8)

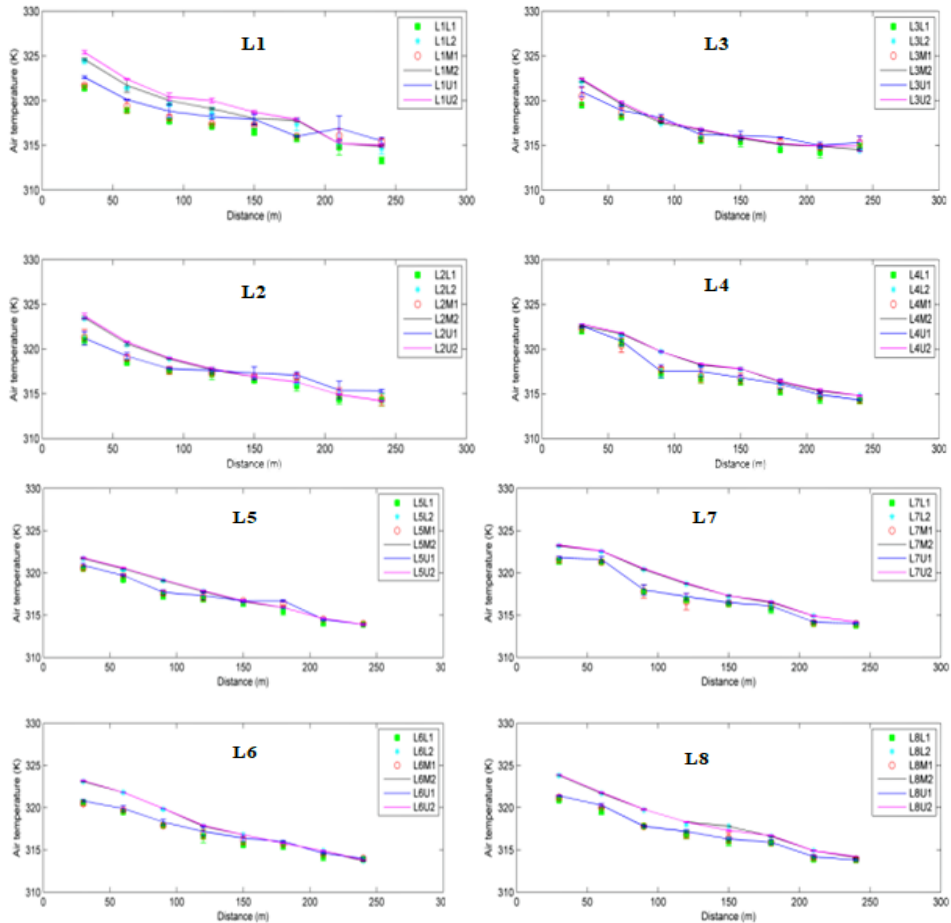


Figure 6: Air temperature at Onne Flow Station (L1-L8)

Table 5: Range, difference and mean of LST from Landsat 5 TM and Landsat 7 ETM+ data, and range, difference and mean of AT measured in the field.

S/N	Flaring site	Land Surface Temperature (K)			Air Temperature (K)		
		Range	Difference (δ LST)	Mean	Range	Difference (δ AT)	Mean
1	Eleme II	279-323	44.0	312.0	313.7-323.9	10.2	318.3
2	Onne	282-320	38.0	309.0	313.9-323.3	9.4	319.0

Generally, for Eleme Refinery II, Figure 5, show that AT from 2012 fieldwork are lower than that of 2019 measurements for all the 8 transect lines. For Onne Flow Station (Figure 6), the AT measured varies, though the 2019 values are higher than that of 2012.

Comparison of LST Retrieved from Atmospherically Corrected Landsat 5 TM and Landsat 7 ETM+ Data with the Measured AT

The range, difference (δ LST) and mean of LST values retrieved from Landsat data, and the range, difference (δ AT) and mean of AT measured on both sites are presented in Table 5.

Table 5 shows that LSTs derived from Landsat data and in-situ data AT agreed to between 0.8-6.0 K. Validation of Landsat-derived LST retrieved was not possible due to lack of in-situ data.

Comparison of Spatial Variability in Ground Air Temperature and Derived LST from Landsat 5 TM and Landsat 7 ETM+ data.

A comparison of spatial variability in ground AT recorded at Eleme Refinery II and Onne Flow Station with their derived LSTs from Landsat data was carried out. The range of AT (δAT) is compared with the range of LST (δLST). From Table 5, the mean (δAT) for Eleme Refinery II and Onne Flow Station are 10.2 K and 9.4 K respectively, while their (δLST) values are 44.0 K and 38.0 K respectively. The difference between the two (δLST) values can be attributed to factors such as rate and volume of burning gas, human activities such as bush burning for the preparation for planting of crops and the atmospheric conditions at the time of satellite overpass.

The Landsat derived LSTs from 1987 to 2013 was plotted together with the in-situ AT for comparison; black lines show the retrieved LSTs and red plot show the AT (Figure 7). The results show that the AT is higher than most of the calculated Landsat LST values and that the AT has a different spatial distribution from LST. However, LST is not exactly the same as AT. Satellite-derived LST is influenced by atmospheric effects while AT was measured in-situ, i.e. with no need to apply an atmospheric correction. The physical parameters for LST and AT are different; radiation from the flare, sun and land heats the air at a different rate (heat capacities). Given, the different processes affecting LST and AT; and the fact that both measurements are within a few K of each other suggests that the techniques are consistent and that the spatial distributions in LST are reliable. The calculated LST and AT results for both sites show similar trend. The in-situ datasets when compared to the LST retrieved show that the spatial distributions for both LST and AT are in good agreement to within 0.8 to 6.0 K. Comparison of this result to other previous literature on retrieval of LST from Landsat data also show good agreement. For example, Coll et al. (2010) results are -0.6 to 1.4 K and -1.8 and 1.3 K; Otukei and Blaschke (2012) result is 0.71 K and Ifatimehin and Adeyemi (2008) recorded a difference of 9.6 K.

Conclusions and Summary

This study provides baseline data on the power of field survey data coupled with satellite imagery for mapping flaring sites in the Niger Delta region; and provide updates for LULC and features retrieved from satellites data. The results from ground measurements have shown the spatial pattern of AT at Eleme Refinery II and Onne Flow Station. The use of 8 lines radiating from the flares to cover the surrounding area of the flare source allowed spatial patterns in AT to be identified (Figure 2). The meteorological data (air temperature) showed that during the period of fieldwork, the background AT recorded were lower because it was the season of highest rainfall

in Nigeria. The AT measured at both sites (Table 3) is higher than AT (298.2 K and 298.7 K) (Table 2) reported by meteorological record for the months of field work (August to September, 2012, and August to September, 2019) respectively.

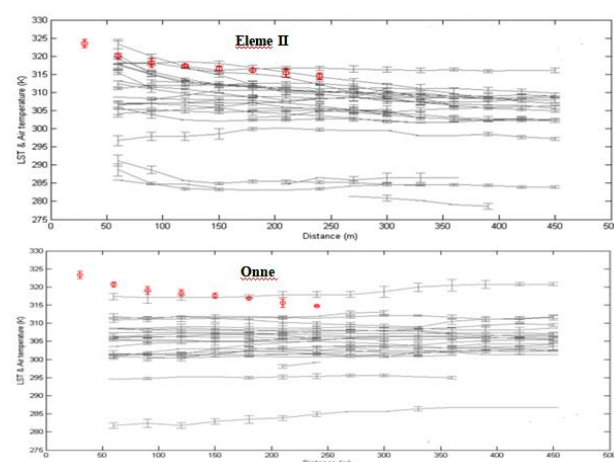


Figure 7: Landsat LST and Air Temperature at Eleme Refinery II and Onne Flow Station

The conversion of AT to get LST will be a useful piece of research to undertake e.g. a sub-pixel scale radiative transfer model. The comparison of this result with the LST from satellite data, such as Landsat data, will help with comparisons of the spatial variability of the impact of flaring at these sites. Also, such future studies can be used to develop geospatial information systems (GIS) technology for flaring sites in the Niger Delta environment; and will ultimately provide insight into the processes of converting AT to LSTs.

Based on the results from Figures 4-7 and Tables 4-5, ground validation of Landsat 5 TM and Landsat 7 ETM+ data through the measurement of in-situ data has made provision for assessment of locational error for points and clarification of features mapped from Landsat data; ascertaining of LULC types; and shows the spatial variability in AT and LSTs retrieved. Also, LSTs retrieved from Landsat data and the in-situ AT shows that the closer the distance to the flare, the higher the temperature and vice versa. Therefore, it can be concluded that ground based measurements is indispensable to validation of satellite data such as Landsat TM and Landsat 7ETM+ data. Ground validation is essential and required for maximum utilization and exploitation of remote sensing technology applications especially at gas flaring sites in the Niger Delta, Nigeria.

Finally, lack of direct and open access for the measurement of in-situ data at oil and gas facility sites in the Niger Delta is a serious challenge. Therefore, Nigerian government should make provisions for policies that enforce multi-national oil companies to allow access to their oil and gas exploration and exploitation sites by the general public especially to research institutions, stakeholders and organizations involved in oil and gas business. The provision of an

enabling environment and sufficient funding for scientific research on oil and gas related disciplines such as gas flaring; and to fully assess its impacts on vegetation, biodiversity and ecosystem, and ensure ways of mitigation is also recommended.

Acknowledgements

We are grateful to USGS for the provision of Landsat imagery and MODTRAN ATMCORR Calculator; and also to Jill Schwarz for guidance and MATLAB coding.

References

- Al-Abdulrazzak, D., Pauly, D. (2014). Ground-truthing the Ground-truth: Reply to Garibaldi et al.'s Comment on "Managing Fisheries from space: Google Earth Improves Estimates of Distant Fish Catches". *ICES Journal of Marine Science* 71: 1927-1931.
- Avşar, E., Bozkurtoğlu, E., Aydar, U., Şeker, D., Kaya, Ş., Gazioglu, C. (2016). Determining Roughness Angle of Limestone Using Optical Laser Scanner. *International Journal of Environment and Geoinformatics*, 3(3), 57-75, doi. 10.30897/ijegeo.306482
- Barsi, J. A., Schott, J. R., Palluconi, F. D., Hook, S. J. (2005). Validation of a Web-Based Atmospheric Correction Tool for Single Thermal Band Instruments. *Earth Observing Systems X*, Proceedings of SPIE Bellingham, WA, 2005.
- Brown, K. (1996). The Utility of Remote Sensing Technology in Monitoring Carbon Sequestration Agroforestry Projects. Forest Carbon Monitoring Program. College of Forest Resources, University of Washington, Washington. 22p.
- Büyüksalih, İ., Gazioglu, C., Gürcan, Büyüksalih, Muftuoglu, AE., Demir, V. (2009). Object-oriented image analysis method of using in Coastal Zone, The Ninth International Conference on the Mediterranean Coastal Environment, 1-10.
- Chander, G., Markham, K. (2003). Revised Landsat-5 TM Radiometric Calibration Procedures and Post-calibration Dynamic Ranges. *IEEE Transactions on Geoscience and Remote Sensing* 41(11): 2674-2677.
- Chen, F., Zhao, X., Ye, H. (2012). Making Use of Landsat 7 SLC-off ETM+ Image through Different Recovering Approaches. Postgraduate Conference on Infrastructure and Environment (3rd IPCIE), vol. 2: 557-563. doi.org/10.5772/48535
- Coll, C., Galve, J. M., Sanchez, J. M., Caselles, V. (2010). Validation of Landsat 7 ETM+ Thermal-band Calibration and Atmospheric Correction with Ground-based Measurement. *IEEE Transaction on Geosciences and Remote Sensing* 48(1): 547-555.
- Celik, B., Kaya, Ş., Alganci, U., Seker, DZ. (2019). Assessment of the relationship between land use/cover changes and land surface temperatures: a case study of thermal remote sensing, *FEB Fresenius Environ. Bull.*, 3, 541
- Dung, E. J., Bombom, L. S., Agusomu, T. D. (2008). The Effects of Gas Flaring on Crops in the Niger Delta, Nigeria. *GeoJournal* 73: 297-305.
- Esetlili, M., Bektas Balcik, F., Balik Sanli, F., Kalkan, K., Ustuner, M., Goksel, C., Gazioglu, C., Kurucu, Y. (2018). Comparison of Object and Pixel-Based Classifications For Mapping Crops Using Rapideye Imagery: A Case Study Of Menemen Plain, Turkey. *International Journal of Environment and Geoinformatics*, 5(2), 231-243, doi. 10.30897/ijegeo.442002
- Franklin, S. E. (1991). Topographic Data and Satellite Spectral Response in Subarctic High-relief Terrain Analysis, *Arctic* 44(1): 15-20.
- Garibaldi, L., Gee, J., Sachiko, T., Mannini, P., Currie, D. (2014). Comment on: Managing Fisheries from Space: Google Earth Improves Estimates of Distant Fish Catches by Al-Abdulrazzak and Pauly. *ICES Journal of Marine Science* 71: 1921-1926
- Gazioglu, C. (2017). Assessment of Tsunami-related Geohazard Assessment for Coasts of Hersek Peninsula and Gulf of İzmit. *International Journal of Environment and Geoinformatics*, 4(2), 63-78, doi. 10.30897/ijegeo.312554
- Gazioglu C., Gökaşan E, Algan O, Yücel, ZY, Tok B, Doğan E (2002) Morphologic features of the Marmara Sea from multibeam data. *Mar Geol* 190:397-420.
- Ifatimehin, O. O., Adeyemi, S. (2008). A Satellite Remote Sensing Based Land Surface Temperature Retrieval from Landsat TM. *Ethiopian Journal of Environmental Studies and Management* 1 (3): 63-70.
- Islam, K., Jasimuddin, M., Nath, B., Nath, T. (2016). Quantitative Assessment of Land Cover Change Using Landsat Time Series Data: Case of Chunati Wildlife Sanctuary (CWS), Bangladesh. *International Journal of Environment and Geoinformatics*, 3(2), 45-55, do.10.30897/ijegeo.306471
- Kaufman, Y. J., Karnieli, A, Tanre, D. (2000). Detection of Dust Over Deserts Using Satellite Data in the Solar Wavelengths. *IEEE Transactions on Geoscience and Remote Sensing* 38: 525-531.
- Maaharjan, A. (2018). "Land use/Land Cover of Katmandu Valley by Using Remote Sensing and GIS". M.Sc. Dissertation Submitted to Central Department of Environmental Science, Institute of Science and Technology, Tribhuvan University, Kirtipur, Kathmandu, Nepal.
- Matthews, S. B. (1991). An Assessment of Bison Habitat in the Mills/Mink Lakes Area, Northwest Territories, Using Landsat Thematic Mapper Data. *Arctic* 44, suppl. 1: 75-80.
- Metz, M., Andreo, V., Neteler, M. (2017). A New Fully Gap-Free Time Series of Land Surface Temperature from MODIS LST Data. *Remote Sensing* 9, 1333.
- Militino, A. F., Ugarte, M. D., Pérez-Goya, U. (2018). Improving the Quality of Satellite Imagery Based on Ground-Truth Data from Rain Gauge Stations. *Remote Sensing*, 1-16.
- Morakinyo, B. O., Lavender, S., Abbott, V. (2019). Mapping of Land Cover and Estimation of their Emissivity Values for Gas Flaring Sites in the Niger Delta. *British Journal of Environmental Sciences* 7 (2): 31-58.

- Morakinyo, B. O. (2015). Flaring and Pollution Detection in the Niger Delta using Remote Sensing. Ph.D Thesis, School of Marine Science and Engineering, University of Plymouth, Plymouth, United Kingdom.
- NASA. (2002). National Aeronautics and Space Administration. Landsat 7 ETM+ Science Data Users Handbook.
- Otukei, J. R., Blaschke, T. (2012). You Know The Temperature at the Weather Station But Do You Know It Anywhere Else? Assessing Land Surface Temperature Using Landsat ETM+ Data. In Proceedings of The first Conference on *Advances in Geomatics Research*.
- Pareta, K. (2014). Land Use and Land Cover Changes Detection Using Multi-temporal Satellite Data. *International Journal of Management and Social Sciences Research* 3(7): 10-17.
- Pressler, R. R., Walker, D. B. (1999). Integrating Deep Tow and Conventional 3D Seismic For Deepwater Seafloor Imaging. *Offshore* 59(7): 98-99.
- Qin, Q., Zhang, N., Nan, P., Chai, L. (2011). Geothermal Area Detection Using Landsat ETM+ Thermal Infrared Data and Its Mechanistic Analysis: A Case Study in Tengchong, China. *International Journal of Applied Earth Observation and GeoInformation* 13: 552-559.
- Sadd, J. L., Hall, E. S., Pastor, M., Morello-Frosch, R. A., Lowe-Liang, D., Hayes, J., Swanson, C. (2015). Ground-Truthing Validation to Assess the Effect of Facility Locational Error on Cumulative Impacts Screening Tools. *Journal of Geography* 2015.
- Serpetti, N., Heath, M., Armstrong, E., Witte, U. (2011). Blending Single Beam RoxAnn and Multi-beam Swathe QTC Hydro-acoustic Discrimination Techniques for the Stonehaven Area, Scotland, UK. *Sea Research* 65(4): 442-455.
- Smith, K., Loughlin, S., Vye, C., Ager, G. (2009). The Application of Thermal Remote Sensing for the Enhanced Mapping and Monitoring of Volcanic Terrain. In *Proceedings of RSPSoc 2009 Annual Conference*, 8-11th September 2009, Leicester, UK (Nottingham).
- Sutariya, S., Hirapara, A., Meherbanali, M., Tiwari, M., Singh, V., Kalubarme, M. (2021). Soil Moisture Estimation using Sentinel-1 SAR Data and Land Surface Temperature in Panchmahal District, Gujarat State. *International Journal of Environment and Geoinformatics*, 8(1), 65-77, doi.10.30897/ijegeo.777434
- Thomas, G. W., Peate, I. U., Nakamoto, J., Pudenz, E., Glasgow, J., Bretthauer, J., Cabrol, N., Wettergreen, D., Grin, E., Coppin, P., Dohm, J. M., Piatek, J. L., Warren-Rhodes, K., Hock, A. N., Weinstein, S., Fisher, G., Chong D. G., Cockell, C., Marinangeli, L., Minkley, N., Moersch, J., Ori, G. G., Smith, T., Stubb, K., Wagner, M., Waggoner, A. S. (2007). Comparing Different Methods for Assessing Ground Truth of Rover Data Analysis for the 2005 Season of the Life in the Atacama Project. *Journal of Geophysical Research* 112.
- Vega, M. B., Craig, M., Lindo, G. A. (2011). Ground Truthing of Remotely Identified Fortifications on the Central Coasts of Peru. *Archaeological Science* 38(7): 1680-1689.
- Yeboah, F., Awotwi, A., Korkuo, E. K. (2017). Assessing the Land Use and Land Cover Changes Due to Urban Growth in Accra, Ghana. *Journal of Basic and Applied Research International* 22(2): 43-50.